THE PROBLEM OF THE SUDDEN MOVEMENT OF A WEDGE

V. V. Titarenko

UDC 533.6.011

The problem of the sudden movement of a wedge with a constant velocity in a medium at rest is examined. Certain cases of the problem have been investigated in a linear approximation in [1-4]. Nonlinear solutions which are valid in the neighborhood of the wave boundary of the perturbation domain have also been constructed in [4]. Nonlinear solutions in the neighborhood of a wedge nose are constructed below for the symmetric and nonsymmetric cases of its low speed motion. The strong qualitative distinction between the isobar fields calculated by the linear and nonlinear theories is shown. In the nonsymmetric case it is found that additional terms must be inserted in the acoustics expansion and in the expansion that is valid in the neighborhood of the wave boundary; their order and form are indicated. The mode of movement with the formation of a hanging shock is detected and the intensity is computed. Linear and nonlinear analyses of all possible cases of the movement of a concave angle are also performed.

1. Let us examine the sudden movement of an infinite wedge of arbitrary apex angle $2\alpha = \alpha_1 + \alpha_2$ (Fig. 1) into an ideal gas at rest at the low constant velocity $w_0 = a_0 M_0$ (a_0 is the sound speed in the gas, $M_0 \ll 1$). Let us introduce a polar system of self-similar coordinates r, θ, whose origin agrees with the wedge nose; the axis $\theta = 0$ is opposite to the direction of wedge motion, and the dimensionless relative excess pressure P and the velocity potential f are:

$$r\cos\theta = x/(a_0 t), \quad r\sin\theta = y/(a_0 t), \quad p = p_0(1 + \gamma P),$$
$$\Phi = a_0^2 t f(r, \theta). \tag{1.1}$$

Here t is the time, p is the pressure, and Φ is the dimensional velocity potential.

The problem of seeking f, P in the perturbation domain OABCDO (Fig. 1) and the position of its boundary is complicated (the formulation is presented in [4], for instance).

Let us take the wedge Mach number M_0 as the small parameter ε of the problem, and let us represent f and P in the form of asymptotic series in ε

$$f = \varepsilon f^{(1)} + \varepsilon^2 f^2 + O(\varepsilon^3), \quad P = \varepsilon P^{(1)} + \varepsilon^2 P^{(2)} + O(\varepsilon^3). \tag{1.2}$$

The linear solution for $P^{(1)}$ has the form [4]

$$P^{(1)} = \sin\alpha_1 \cdot I\{\sigma^\lambda, \lambda(\theta - \alpha_1), -\lambda\pi/2\} + \sin\alpha_2 \cdot I\{\sigma^\lambda, \lambda(\theta - \alpha_1), \lambda(3\pi/2 - \alpha_1 - \alpha_2)\},$$
$$\lambda = \pi/(2\pi - \alpha_1 - \alpha_2), \quad \sigma = [1 - (1 - r)^{1/2}]r; \tag{1.3}$$

$$I\{a, b, c\} = (1/\pi)\,\mathrm{arctg}\,\{(1 - a^2)\sin c/[2a\cos b - (1 + a^2)\cos c]\}. \tag{1.4}$$

Values of the arctangents in (1.4) are taken in the interval $(0, \pi)$.

The field of isobars $P^{(1)} = \mathrm{const}$ and gradient isolines $P_r^{(1)} = \mathrm{const}$ calculated by means of (1.3) for the angles $\alpha_1 = \alpha_2 = 37.5°$ and $\alpha_1 = 60°$, $\alpha_2 = 15°$ are presented in Fig. 1a-d (the number alongside the lines indicates the value of the constant). Fig. 1 graphically demonstrates the qualitative distinction between the fields P, P_r in the symmetric and nonsymmetric cases and indicates the explicit defects in linear theory in the neighborhood of the wave boundary ABCD of the perturbation domain, and in the neighborhood of the wedge nose in the nonsymmetric case.

2. Let us investigate the flow near the wedge nose. Let us first examine the symmetric case. Let $r \to 0$, we obtain from the linear solution (1.3) for $\alpha_1 = \alpha_2$

Saratov. Translated from Zhurnal Prikladnoi Mekhaniki i Tekhnicheskoi Fiziki, No. 4, pp. 155-165, July-August, 1981. Original article submitted January 25, 1980.

0021-8944/81/2204-0579$07.50

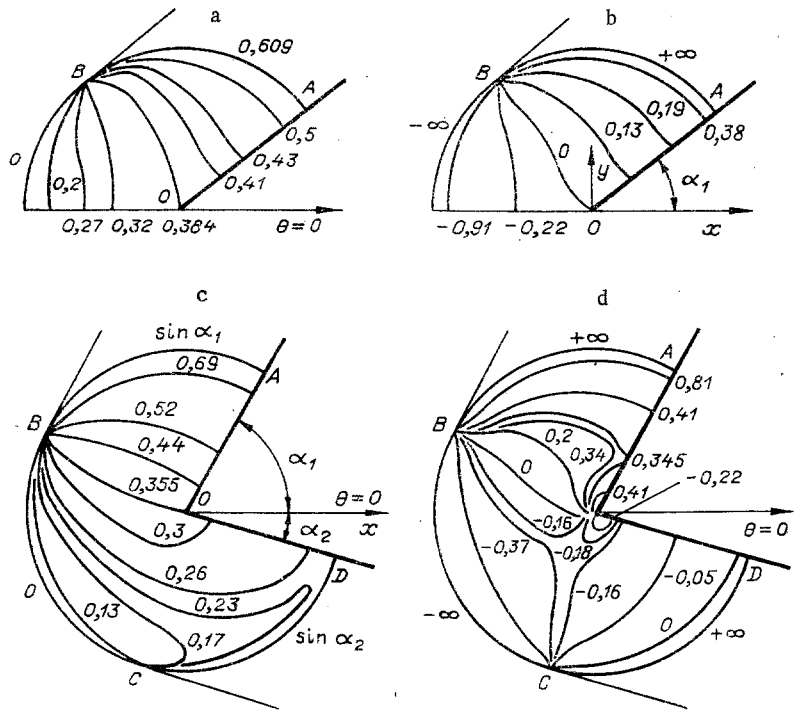

Fig. 1

$$P^{(1)} = \pi_{1*} + \nu_1 r^{2\lambda}\cos 2\omega_1 + \nu_2 r^{4\lambda}\cos 4\omega_1 + o\left(r^{4\lambda}\right),$$
$$\text{where} \quad \pi_{1*} = \lambda(\sin\alpha_1 + \sin\alpha_2)/2;$$
$$\lambda = \pi/(2\pi - \alpha_1 - \alpha_2); \quad \omega_1 = \lambda(\theta - \alpha_1); \quad \pi\nu_1 = 2^{1-2\lambda}\sin\alpha_1 \sin\lambda\pi; \tag{2.1}$$
$$\pi\nu_2 = 2^{-4\lambda}\sin\alpha_1 \sin 2\lambda\pi.$$

Using (2.1) in the equations for the second terms in the expansion (1.2) as $r \to 0$, obtained by the method of the small parameter, we find the expansions of P, f as $r \to 0$

$$P = \pi_* + \varepsilon\{\nu_1 r^{2\lambda}\cos 2\omega_1 + \nu_2 r^{4\lambda}\cos 4\omega_1 + o\left(r^{4\lambda}\right)\} + \varepsilon^2\{g_{21}r^{4\lambda-2} +$$
$$+ g_{22}r^{6\lambda-2} + o\left(r^{6\lambda-2}\right)\} + O(\varepsilon^3), \quad g_{21} = -2[\lambda\nu_1/(2\lambda-1)]^2,$$
$$g_{22} = -8\lambda^2\nu_1\nu_2\cos 2\omega_1/[(2\lambda-1)(4\lambda-1)],$$
$$f = \varepsilon\{\nu_1 r^{2\lambda}\cos 2\omega_1/(2\lambda-1) + \nu_2 r^{4\lambda}\cos 4\omega_1/(4\lambda-1) + \tag{2.2}$$
$$+ o(r^{4\lambda})\} + \varepsilon^2\{g_2 r^{4\lambda} + o(r^{4\lambda})\} + O(\varepsilon^3),$$
$$\pi_* = \varepsilon\pi_{1*} + \varepsilon^2\pi_{1*}^2/2 + O(\varepsilon^3), \quad g_2 = A\cos 4\omega_1 + \nu_1^2/[2(1-2\lambda)], \; A - \text{const}.$$

According to (2.2), the expansion for P is nonregular [5] for $r \leqslant r_c$, where $r_c \sim \varepsilon \exp\cdot(1/2-2\lambda)$. The inner [5] variables and expansions in the neighborhood of the wedge nose, which is a stagnation point (according to (2.2) the particle velocity is $f_r^2 + r^{-2}f_\theta^2 = 0$ for $f = 0$), we introduce in conformity with (2.2)

$$r = \varepsilon^{1/(2-2\lambda)}s, \quad f = \varepsilon^{1/(1-\lambda)}\chi_1(s,\theta) + \varepsilon^{\lambda_1}\chi_2(s,\theta) + \ldots,$$
$$P = \pi_* + \varepsilon^{1/(1-\lambda)}\Delta_1(s,\theta) + \varepsilon^{\lambda_1}\Delta_2(s,\theta) + \ldots, \quad \lambda_1 = (1+\lambda)/(1-\lambda). \tag{2.3}$$

Substituting (2.3) into the exact equations of the problem, we obtain that the parameters in the neighborhood r = 0 are determined in the first two approximations from the situations of the equations of incompressible fluid motion

$$\nabla^2\chi_1 = \chi_{1ss} + \chi_{1s}/s + \chi_{1\theta\theta}/s^2 = 0, \quad \Delta_1 = s\chi_{1s} - \chi_1 - (\chi_{1s}^2 + \chi_{1\theta}^2/s^2)/2; \tag{2.4}$$

$$\nabla^2\chi_2 = 0, \; \Delta_2 = s\chi_{2s} - \chi_2 - \chi_{1s}\chi_{2s} - \chi_{1\theta}\chi_{2\theta}/s^2. \tag{2.5}$$

The boundary value problems to determine χ_1, χ_2 include (2.4), (2.5), conditions on the

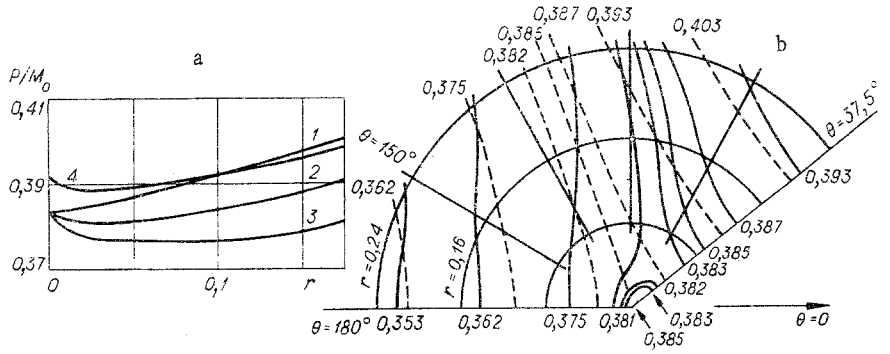

Fig. 2

wedge surface and the line of symmetry

$$\chi_{1\theta} = \chi_{2\theta} = 0 \text{ при } \theta = \alpha_1,\ \theta = \pi,\ 0 \leqslant s \leqslant s_0,\ s_0 \to \infty \tag{2.6}$$

and the condition for merger with the acoustics solutions (1.2), (2.2) which are valid far from the nose as $s \to \infty$. These latter are obtained by equilibration of the outer expansion of f of order $O(\varepsilon^3)$, of the inner expansion of f (2.3) of order $O(\varepsilon^{\lambda_1})$ (in abbreviated form $\left(f_i^{\varepsilon^{\lambda_1}}\right)_0^{\varepsilon^2}$) and the inner expansion of f of order $O(\varepsilon^{\lambda_1})$ of the outer expansion of f (2.2) of order $O(\varepsilon^2)$ (in abbreviated form $\left(f_0^{\varepsilon^2}\right)_i^{\varepsilon^{\lambda_1}}$). We have here from (2.2) and (2.3)

$$\left(f_0^{\varepsilon^2}\right)_i^{\varepsilon^{\lambda_1}} = \varepsilon^{1/(1-\lambda)} v_1 s^{2\lambda} \cos 2\omega_1/(2\lambda - 1) + \varepsilon^{\lambda_1} v_2 s^{4\lambda} \cos 4\omega_1/(4\lambda - 1).$$

The general solutions for χ_1, χ_2 can be obtained by separation of variables, and they are presented in [6]. We obtain solutions of the boundary value problems for χ_1, χ_2, that satisfy conditions (2.6) and the merger conditions by the general solutions from [6]. It is convenient to write the final answers by introducing the plane of a complex variable and complex potentials:

$$z = se^{i\theta},\ W_1(z) = \chi_1(s, \theta) + i\psi_1(s, \theta),\ W_2(z) = \chi_2(s, \theta) + i\psi_2(s, \theta) \tag{2.7}$$

(ψ_1, ψ_2 are stream functions). They then become

$$W_1 = v_1 \left(ze^{-i\alpha_1}\right)^{2\lambda}/(2\lambda - 1),\ \Delta_1 = v_1 s^{2\lambda} \cos 2\omega_1 + g_{21} s^{4\lambda - 2}; \tag{2.8}$$

$$W_2 = v_2 \left(ze^{-i\alpha_1}\right)^{4\lambda}/(4\lambda - 1),\ \Delta_2 = v_2 s^{4\lambda} \cos 4\omega_1 + g_{22} s^{6\lambda - 2}. \tag{2.9}$$

Computations using (2.3), (2.8) and (2.9) are presented in Fig. 2. The pressure distribution $P^{(1)}$ over the surface of a wedge with angles $\alpha_1 = \alpha_2 = 37.5°$ moving in air is represented in Fig. 2a. From linear theory (curve 1) the pressure at the nose is minimal. From nonlinear theory (curves 2-4 correspond to monomial for $M_0 = 0.1$, monomial for $M_0 = 0.2$, and binomial for $M_0 = 0.1$ inner solutions), on the wedge surface there are two minimum P points located symmetrically at a short range from the nose, at which there is a local maximum P. The nonlinear isobar field $P^{(1)} = \text{const}$, evaluated for $\varepsilon = M_0 = 0.1$ by the mononmial inner solution (solid curves in Fig. 2b), differs in principle, from the field predicted by linear theory (Fig. la, and the dashed curves in Fig. 2b).

3. In the case of nonsymmetric wedge motion, we obtain from (1.3) as $r \to 0$

$$P^{(1)} = \pi_{1*} + \mu_1 r^{\lambda} \cos \omega_1 + \mu_2 r^{2\lambda} \cos 2\omega_1 + o\left(r^{2\lambda}\right), \tag{3.1}$$

where

$$\pi\mu_1 = -2^{1-\lambda}(\sin \alpha_2 - \sin \alpha_1) \sin (\lambda\pi/2);$$
$$\pi\mu_2 = 2^{-2\lambda}(\sin \alpha_1 + \sin \alpha_2) \sin \lambda\pi.$$

By using (3.1) in the equations for $f^{(2)}$, $P^{(2)}$ as $r \to 0$, we find the expansions of f, P as $r \to 0$

$$P=\pi_*+\varepsilon\{\mu_1 r^\lambda\cos\omega_1+\mu_2 r^{2\lambda}\cos 2\omega_1+o\left(r^{2\lambda}\right)\}+\varepsilon^2\{h_{21}r^{2\lambda-2}+h_{22}r^{3\lambda-2}+$$
$$+o\left(r^{3\lambda-2}\right)\}+O(\varepsilon^3),\ 2h_{21}=-[\lambda\mu_1/(\lambda-1)]^2,\ h_{22}=-2\lambda^2\mu_1\mu_2\cos\omega_1/[(\lambda-$$
$$-1)(2\lambda-1)],\ f=\varepsilon\{\mu_1 r^\lambda\cos\omega_1/(\lambda-1)+\mu_2 r^{2\lambda}\cos 2\omega_1/(2\lambda-1)+$$
$$+o\left(r^{2\lambda}\right)\}+\varepsilon^2\{h_2 r^{2\lambda}+o\left(r^{2\lambda}\right)\}+O(\varepsilon^3),\ h_2=A_1\cos 2\omega_1+$$
$$+\mu_1^2/[2(1-\lambda)],\ A_1-\text{const}. \tag{3.2}$$

According to (3.2), the expansion for P is not regular for $r \leqslant r_H$, where $r_H \sim \varepsilon^{1/(2-\lambda)}$. The inner variables and expansions in the neighborhood of r = 0 are introduced in conformity with (3.2)

$$r=\varepsilon^{1/(2-\lambda)}s,\ f=\varepsilon^{2/(2-\lambda)}\chi_1(s,\theta)+\varepsilon^{\lambda_2}\chi_2(s,\theta)+\ldots,$$
$$P=\pi_*+\varepsilon^{2/(2-\lambda)}\Delta_1(s,\theta)+\varepsilon^{\lambda_2}\Delta_2(s,\theta)+\ldots,\ \lambda_2=(2+\lambda)/(2-\lambda). \tag{3.3}$$

Substituting (3.3) in the exact equations, we obtain the inner equations (2.4) and (2.5).

The domain of unsuitability of the acoustics expansions in the nonsymmetric case is considerably greater than in the symmetric case. According to (3.2), P_r and the particle velocity grow without limit as $r \to 0$, which indicates the overflow of gas particles from one wedge fact to another (from the upper to the lower in Fig. 1d). But as is known [7, 8], such a process should be accompanied by formation of a vortex which would smooth a sharp edge to assure a finite particle velocity.

The construction of a vortex flow in the neighborhood of the nose can be executed under the assumptions [8-11]: 1) inviscid flow; 2) the vorticity is concentrated in the vortex sheet, a surface of tangential velocity discontinuity starting at the nose and curving into a certain spiral (the shape of the spiral is unknown, while the flow outside the sheet is potential).*

In this case the complex flow potential can be represented in the form $W_1 = W_{11} + W_{12}$, where W_{11} is the potential of the unseparated flow around the nose by the incompressible fluid, and W_{12} is the potential of the sheet. Analogously $\Delta_1 = \Delta_{11} + \Delta_{12}$.

We find the expressions for W_{11} and W_2 by a known method [7, 8]:

$$W_{11}=b_1\left(ze^{-i\alpha_1}\right)^\lambda,\ W_2=b_2\left(ze^{-i\alpha_1}\right)^{2\lambda},\ b_1, b_2-\text{const}. \tag{3.4}$$

We determine the arbitrary constants b_1, b_2 as a result of merger with the acoustic solution.

Let us turn to finding W_{12}. Let $z_N = s_N\exp(i\theta_N)$ determine the location of a certain point of the sheet. Instead of the physical circulation $C(r, \theta, t)$ we introduce the dimensionless circulation $\varkappa(s,\theta)=C/\left(a_0^2 t\right)$ because of self-similarity. The complex potential of a point vortex at the point z_N and with intensity $\varkappa_N$ can be obtained by a conformal mapping of the flow domain on the upper half-plane by using the known solution [10] for a point vortex and taking account of the presence of the wall

$$W_N=i\varkappa_N/(2\pi)\,\mathrm{Ln}\left\{\left(z^\lambda-z_N^\lambda\right)/\left(z^\lambda-e^{2i\alpha_1\lambda}\overline{z_N^\lambda}\right)\right\}. \tag{3.5}$$

Here and henceforth, the bar above will denote the complex-conjugate.

Denoting the arclength of the sheet measured from the wedge nose by l we obtain W_{12} by the superposition of point vortices (3.5):

$$W_{12}=i/(2\pi)\int_0^l \mathrm{Ln}\left\{\left(z^\lambda-z_l^\lambda\right)/\left(z^\lambda-e^{2i\alpha_1\lambda}\overline{z_l^\lambda}\right)\right\}d\varkappa_l. \tag{3.6}$$

The velocity potential of the sheet is $\chi_{12} = \mathrm{Re}\{W_{12}\}$, and the pressure Δ_{12} is found from the second equation in (2.4).

*We neglect the possibility of secondary (etc.) stream separation caused by the main vortex.

Finding x_l and z_l should evidently be done under specific conditions, namely: the Kutta–Zhukovskii conditions of finiteness of the velocity at the wedge nose, the conditions for no strong effect on the sheet (equality of the pressures and the particle velocity components normal to the sheet on both its sides), and conditions formulated for the total velocity potential W_1 and the pressure Δ_1 on the wedge surface.

The solution of this complicated problem can be obtained numerically (a survey of different methods is given in [11]).

In this case we are interested in another question, not touched upon earlier, about the agreement between the vortex flow and the flow far from the nose of the wedge.

For a fixed inner variable s the limit process $\varepsilon \to 0$ means that $r \to 0$ according to (3.3). Therefore according to (1.2), (3.2), and (3.3).

$$\left(f_0^{\varepsilon^2}\right)_i^{\varepsilon^{\lambda_2}} = \varepsilon^{2/(2-\lambda)}\mu_1 s^{\lambda}\cos\omega_1/(\lambda-1) + \varepsilon^{\lambda_2}\mu_2 s^{2\lambda}\cos 2\omega_1/(2\lambda-1). \tag{3.7}$$

For a fixed outer variable s, the limit process $\varepsilon \to 0$, means $r \to 0$ in conformity with (3.3). Then according to (3.3), (3.4), and (3.6), as $z \to \infty$.

$$\left(f_i^{\varepsilon^{\lambda_2}}\right)_0^{\varepsilon^2} = \varepsilon^{2/(2-\lambda)}\left[b_1 s^{\lambda}\cos\omega_1 + (T/s^{\lambda})\cos\omega_1\right] + \varepsilon^{\lambda_2} b_2 s^{2\lambda}\cos 2\omega_1; \tag{3.8}$$

$$T = (1/\pi)\int_0^l s_l^{\lambda}\sin\omega_{1l}\,dx_l,\ \omega_{1l} = \lambda(\theta_l - \alpha_1). \tag{3.9}$$

Equating the outer (3.7) and inner (3.8) limits, we obtain

$$b_1 = \mu_1/(\lambda-1),\ b_2 = \mu_2/(2\lambda-1). \tag{3.10}$$

A term which has not merged, which is the asymptotic of the vortex sheet, here remains in (3.8). Hence, additional terms taking account of the vortical nature of the flow in the neighborhood of the wedge nose must be inserted in the outer expansion of (1.2). According to (3.8), (3.7) and (3.3), the acoustics expansions should have the form

$$\begin{aligned} f &= \varepsilon f^{(1)} + \varepsilon^{\lambda_2} f^* + \varepsilon^2 f^{(2)} + o(\varepsilon^2, \varepsilon^{\lambda_2}), \\ P &= \varepsilon P^{(1)} + \varepsilon^{\lambda_2} P^* + \varepsilon^2 P^{(2)} + o(\varepsilon^2, \varepsilon^{\lambda_2}). \end{aligned} \tag{3.11}$$

The equations f*,p* agree outwardly with the equations for $f^{(1)}, p^{(1)}$

$$(1-r^2)f^*_{rr} + r^{-1}f^*_r + r^{-2}f^*_{\theta\theta} = 0,\ P^* = rf^*_r - f^*. \tag{3.12}$$

Eliminating f* from the system of equations (3.12) and applying the Busemann-Chaplygin transformation $\sigma = [1-(1-r^2)^{1/2}]/r$, $\theta = 0$, we obtain a Laplace equation for P*. Furthermore, applying conformal mapping, we reduce the boundary value problem to determine P* to a Dirichlet problem in the plane $\sigma_2 = \sigma^{\lambda}$, $\theta_2 = \lambda(\theta - \alpha_1)$ for a half-ring $\varepsilon_1 \leqslant \sigma_2 \leqslant 1$, $0 \leqslant \theta_2 \leqslant \pi$, $\varepsilon_1 \to 0$. Evidently P* = 0 for $0 \leqslant \theta_2 \leqslant \pi$, $\sigma_2 = 1$; $P^*_{\theta} = 0$ for $\varepsilon_1 \leqslant \sigma_2 \leqslant 1$, $\theta_2 = 0$, $\theta_2 = \pi$. According to (3.8), (3.3), (3.12), for $\sigma_2 = \varepsilon_1$, $0 \leqslant \theta_2 \leqslant \pi$, $P^* = -(\lambda+1)T\cos\omega_1/(\varepsilon_1 2^{\lambda})$.

The solution of this boundary value problem has the form

$$P^* = (\lambda+1)2^{-\lambda}T(\sigma^{\lambda} - \sigma^{-\lambda})\cos\omega_1. \tag{3.13}$$

The potential f* is found from (3.12).

4. Let us construct an approximate model of the vortex flow that permits obtaining simple analytical formulas to estimate the influence of a vortex on the flow field.

Let us replace the vortex sheet by a single point vortex (3.5), where the x_N, s_N, θ_N are unknown. Such a model was used in investigating other problems, for instance, in [12, 8, 13]. In this case it is necessary to connect the point N and the wedge nose by a straight-line segment and to superpose a Zhukovskii force on the segment-isolated vortex system so that the

resultant force in the system would be zero [8, 12, 13]. Taking self-similarity into account, this yields

$$V_{z_N} = 2\bar{z}_N. \tag{4.1}$$

On the other hand, $V_{zN} = dW_1/dz$ for $z = z_N$, where $W_1 = W_{11} + W_{12}$. According to (3.5), $dW_{12}/dz = dW_N/dz$ has a simple pole at $z = z_N$. By assumption [10], the particle velocity at a singularity is defined as the regular part of dW_1/dz at this point. Therefore

$$V_{z_N} = \lim_{z \to z_N} \{dW_1/dz - i\varkappa_N/[2\pi(z - z_N)]\}.$$

Expanding this latter limit by L'Hopital's rule, we obtain

$$V_{z_N} = \lambda b_1 e^{-i\alpha_1\lambda} z_N^{\lambda-1} + i\varkappa_N\left[(\lambda - 1)/(2z_N) - \lambda z_N^{\lambda-1}\Big/\left(z_N^{\lambda} - e^{2i\alpha_1\lambda}\overline{z_N^{\lambda}}\right)\right]\Big/(2\pi). \tag{4.2}$$

Separating real and imaginary parts of the expression obtained by equating (4.1) and (4.2), we find

$$s_N = \left(-\frac{\lambda}{2}\mu_1 \cos\omega_{1N}\right)^{1/(2-\lambda)}, \quad \varkappa_N = 8\pi s_N^2 \operatorname{tg}\omega_{1N}/(1 - \lambda), \quad \text{where} \quad \omega_{1N} = \lambda(\theta_N - \alpha_1). \tag{4.3}$$

We find the last unknown θ from the Kutta–Zhukovskii condition by requiring boundedness of dW_1/dz as $z \to 0$:

$$\theta_N = \alpha_1 + c \quad \text{for} \quad \alpha_1 < \alpha_2, \quad \theta_N = 2\pi - \alpha_2 - c \quad \text{for} \quad \alpha_1 > \alpha_2, \quad \text{where} \quad c = \frac{1}{\lambda}\arcsin\frac{1}{2\sqrt{\lambda}}. \tag{4.4}$$

According to (3.5), the velocity potential of the vortex flow has the form

$$\chi_{12} = -\frac{\varkappa_N}{2\pi}\operatorname{arctg}\frac{s_N^{2\lambda}\sin 2\omega_{1N} - 2s^{\lambda}s_N^{\lambda}\sin\omega_{1N}\cos\omega_1}{s^{2\lambda} - 2s^{\lambda}s_N^{\lambda}\cos\omega_1\cos\omega_{1N} + s_N^{2\lambda}\cos 2\omega_{1N}}. \tag{4.5}$$

We find the pressure Δ_{12} by substituting (4.5) into (2.4).

Computations using (3.3)-(3.5), (3.10), (4.3)-(4.5), and represented in Fig. 3, qualitatively illustrate the influence of vortex formation on the pressure distribution near the wedge nose on the face OA (Fig. 3a) and on the face OD (Fig. 3b). Curves 1-4 in Fig. 3 are respectively calculated by using the linear; the binomial outer, taking account of vortex formation ($\lambda < 2/3$); monomial inner for $M_0 = 0.1$; and monomial composite for $M_0 = 0.1$ solutions. The difference, in principle, between the linear and nonlinear distributions is observed.

Let us note that the quantity T determined in (3.9) and entering into the additional term of the acoustic expansion (3.11) (see (3.13)), takes on the value T_N in the case of a point vortex model

$$T_N = (\varkappa_N/\pi)\, s_N^{\lambda}\sin\omega_{1N}. \tag{4.6}$$

Let us also note that the relationship to determine $\varkappa_\zeta$, s_ζ, θ_ζ, that follows from the Kutta–Zhukovskii condition for W_1 with W_{11} and W_{12} determined in (3.4) and (3.6), has the form $\pi\mu_1 = (\lambda - 1)\int_0^l s_l^{\lambda}\sin\omega_{1l}\, d\varkappa_l$. It goes over into (4.4) upon replacement of the sheet by a point vortex.

5. In the nonsymmetric case, when the movement is accompanied by the origination of a vortex, it follows from (3.11) that it is necessary to induce an addition to the process performed in [4] to construct nonlinear solutions in the neighborhood of the wave boundary ABCD (see Fig. 1).

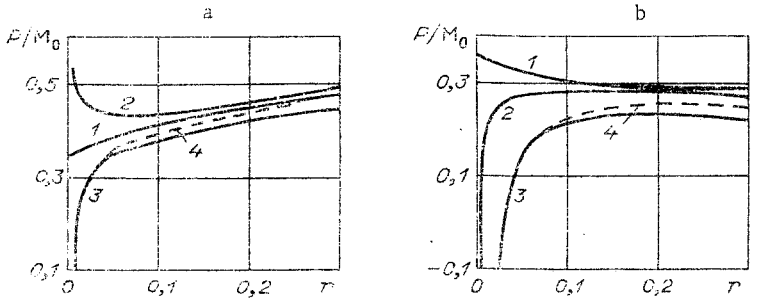

Fig. 3

Let us illustrate this by the example of a shock front BC being propagated in a medium at rest. The expansions (3.11) in the neighborhood of BC take the following form as $r \to 1$, $|\theta - \theta_B| \geqslant (1-r)^{1/2}$, $|\theta - \theta_C| \gg (1-r)^{1/2}$:

$$P = \varepsilon\{d_1\rho^{1/2} + O(\rho^{3/2})\} + \varepsilon^{\lambda_2}\{Q_*\rho^{1/2} + O(\rho^{3/2})\} + \varepsilon^2\{(\gamma+1)d_1^2/2 + O(\rho^{1/2})\} + o(\varepsilon^2, \varepsilon^{\lambda_2}),\ f = \varepsilon\{-2d_1\rho^{3/2}/3 + O(\rho^{5/2})\} + \varepsilon^{\lambda_2}\{-2Q_*\rho^{3/2}/3 + O(\rho^{5/2})\} + \varepsilon^2\{-(\gamma+1)d_1^2\rho/2 + O(\rho^{3/2})\} + o(\varepsilon^2, \varepsilon^{\lambda_2}),\ \rho = 1 - r,$$
$$Q_* = -2^{3/2-\lambda}\lambda(\lambda+1)T\cos\omega_1,\ d_1(\theta) = \lambda\left\{\sin\alpha_1\left[\operatorname{ctg}\frac{\lambda}{2}\left(\theta - \frac{\pi}{2} - \alpha_1\right) - \operatorname{ctg}\frac{\lambda}{2}\left(\theta + \frac{\pi}{2} - \alpha_1\right)\right] + \sin\alpha_2\left[\operatorname{ctg}\frac{\lambda}{2}\left(\theta + \frac{3\pi}{2} - 2\alpha_1 - \alpha_2\right) - \operatorname{ctg}\frac{\lambda}{2}\left(\theta - \frac{3\pi}{2} + \alpha_2\right)\right]\right\}/(\pi\sqrt{2}). \tag{5.1}$$

Near BC we introduce the inner variables according to (5.1):

$$r = 1 - \varepsilon^2 d_1^2\delta,\ P = 2\varepsilon^2 d_1^2\{\Pi_4(\delta,\theta) + \varepsilon^{\lambda_2-1}\Pi^*(\delta,\theta) + \varepsilon\Pi_5(\delta,\theta) + \ldots\}/(\gamma+1),$$
$$f = -2\varepsilon^4 d_1^4\{G_4(\delta,\theta) + \varepsilon^{\lambda_2-1}G^*(\delta,\theta) + \varepsilon G_5(\delta,\theta) + \ldots\}/(\gamma+1). \tag{5.2}$$

The solutions of the equations Π_4, G_4 are presented in [4]:

$$\Pi_4 = (1 + bH)/c_1,\ G_4 = \delta/c_1 + 2Hb^3/(3c_1^2) + c_2,\ b = (1 + \delta c_1)^{1/2}. \tag{5.3}$$

The equations for Π^*, G^* and their solutions have the form

$$\Pi^* = G^*_\delta,\ 2(\Pi_1 + \delta)\Pi^*_\delta + (2\Pi_{4\delta} - 1)\Pi^* = 0; \tag{5.4}$$

$$\Pi^* = ek_3(1 + Hb)^2/b,\ G^* = 2k_3\, eH(1 + Hb)^3/(3c_1) + k_4,\ e = \exp(1). \tag{5.5}$$

Here c_1, c_2, k_3, k_4 are arbitrary functions of θ, and $H = \pm 1$.

The equations for Π_5, G_5 agree outwardly with (5.4).

By merging the expansions (3.11) and (5.2) at the level

$$\left(P_0^{\varepsilon^{\lambda_2}}\right)_i^{\varepsilon^{\lambda_2+1}} = \left(P_i^{\varepsilon^{\lambda_2+1}}\right)_0^{\varepsilon^{\lambda_2}},\ \left(f_0^{\varepsilon^{\lambda_2}}\right)_i^{\varepsilon^{\lambda_2+3}} = \left(f_i^{\varepsilon^{\lambda_2+3}}\right)_0^{\varepsilon^{\lambda_2}},$$

we obtain

$$c_1 = 4/(\gamma+1)^2,\ H = \operatorname{sign}(d_1),\ k_3 e = \operatorname{sign}(d_1)\,Q_*/(c_1 d_1). \tag{5.6}$$

The arbitrary functions and constants in the inner solutions (5.3) and (5.5) are found by satisfying the boundary conditions on the shock front

$$\delta = \delta_* = \delta_0 + \varepsilon^{\lambda_2-1}\delta^* + \varepsilon\delta_1 + \ldots. \tag{5.7}$$

Using (5.2) and (5.7) in the exact conditions, we obtain

$$\Pi_4(\delta_0) = -2\delta_0,\ G_4(\delta_0) = 0; \tag{5.8}$$

$$\delta^*\Pi_{4\delta}(\delta_0) + \Pi^*(\delta_0) = -2\delta^*,\ d_1\delta^{*\prime}\Pi_4(\delta_0) + 4d_1'[\delta^*\Pi_4(\delta_0) + G^*(\delta_0)] = 0 \tag{5.9}$$

(the prime denotes the derivative with respect to θ).

Satisfying (5.8), we find c_2, δ_0, and satisfying (5.9) we find k_4, δ^* (this can be done only for H = 1, i.e., for $d_1 > 0$)

$$c_2 = 2/(3c_1^2),\ \delta_0 = -3/(4c_1),\ \delta^* = -3k_3e/2,$$
$$k_4 = 9d_1(k_3e)'/(16c_1d_1'),\ H = 1. \tag{5.10}$$

It can be seen that the formulas for the highest terms of the expansions (5.2) and (5.7) agree with those obtained in [4]. Formulas (5.5), (5.6), (5.10) for the next terms in the expansions (5.2), (5.7) permit estimation of the influence of vortex formation on the flow parameters near BC.

The vortex formation is taken into account analogously in the valid solutions near the fronts of the weak lines of discontinuity AB and CD. Here $c_2 = k_4 = 0$, $H = \mathrm{sign}(d_1) = -1$ in (5.5) and (5.6).

Let us note that the boundary value problem for the neighborhood of the triple point B, that is formulated in [4], does not change if vortex formation is taken into account since we have $\Pi^* \sim d_1|\theta - \theta_B|$ as $|\theta - \theta_B| \to 0$ from (5.5) and (5.6) and that the inner expansions (5.2) are regular according to (5.2)-(5.7) and (5.10).

6. In addition to the results of [4], let us note the interesting fact from the physical viewpoint: nonsymmetric movement of the wedge at low velocity is accompanied, for certain values of the angles α_1, α_2, by the origination of a hanging shock, going from the wedge face and forming a smaller angle with the axis OX (the face OD in Fig. 1c).

To prove this, let us consider the quantity $H = \mathrm{sign}(d_1)$ by assuming $\alpha_1 \geqslant \alpha_2$ for definiteness. According to Sec. 5, it must be proved that H = 1 at the point D and in some neighborhood. An analysis of d_1 from (5.1) shows that for $\theta = \theta_D = 2\pi - \alpha_2$ the quantity H is $\mathrm{sign}[\sin\alpha_1 \times \sin^2(\lambda\pi/4) - \sin\alpha_2\cos^2(\lambda\pi/4)]$ at the point D. Therefore, a hanging shock DG occurs near the face OD (G is a certain point on the front DC at which the shock degenerates into a line of weak discontinuity) if the initial data of the problem α_1, α_2 belong to the domain $A(\alpha_1, \alpha_2)$, defined by the relationship $\sin\alpha_2\sin^2(\lambda\pi/4) > \sin\alpha_2\cos^2(\lambda\pi/4)$. In the plane $(\alpha_1 + \alpha_2)/\pi$, α_2, the domain A lies below the curve displayed in Fig. 4a (let us note that if $\alpha_1 = \alpha_2$, H = −1 for $\theta_C < \theta \leqslant \theta_D$ while the front CD is always entirely a line of weak discontinuity).

The location and intensity of the shock DG and the parameters behind it can be determined by known formulas [4]. Let us note that the maximum wave intensity is achieved at the point D.

It is interesting that as α_1 changes for a fixed α_2 a qualitative change is observed in the pressure diagram along the face OD. This is illustrated by Fig. 4b, where computations of the pressure P/M_0 along the faces OA, OD are represented (the upper and lower parts of the curves, respectively), which have been executed for $\alpha_2 = 15°$ and $\alpha_1 = 15;\ 30;\ 60;\ 75°$. When the pressure along OD drops monotonically ($\alpha_1 = 75°$), we have a mode with the formation of the hanging shock DG according to Fig. 4a.

7. In conclusion, let us examine the case not investigated in [1-4] of low velocity ($M_0 \ll 1$) movement of a concave aperture angle $2\alpha = \alpha_1 + \alpha_2$ ($2\alpha > \pi$, $\alpha_1 \geqslant \alpha_2$, $\alpha_1 < \pi$). In this case (Fig. 5), reflection of the plane shocks from each other occurs, and if $4\alpha > 3\pi$, from the faces of the angle also. The nature of the interference, i.e., the quantity of front reflections from each other and from the faces, and the magnitude of the parameters in the domains of piecewise-constant values of P depend on M_0, 2α and the relationship between α_1, α_2 and are successively determined by the solution of problems on the collision of plane shocks of different intensity and on shock reflection from a wall [14].

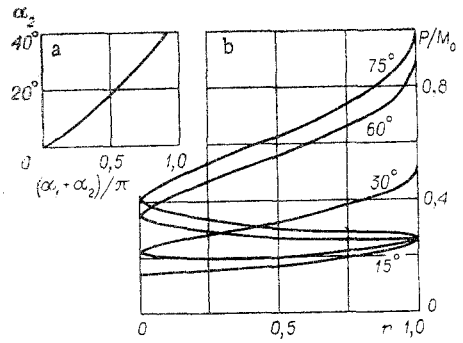

Fig. 4

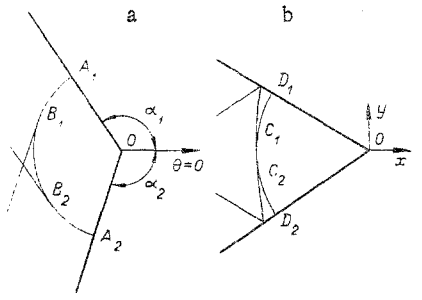

Fig. 5

It can be noted that as α grows the quantity of reflections increases; here one of the situations displayed in Figs. 5a and b is realized alternately in the neighborhood of the wave boundary of the perturbation domain. In a linear approximation, the variation intervals 2α corresponding to the different interference patterns are determined by the relationship

$$(1 + 2n)\pi/(1 + n) < 2\alpha < (3 + 2n)\pi/(2 + n), \; n = 0, 1, 2, \ldots. \tag{7.1}$$

For n = 0, 2, 4, ... (n ∿ is the quantity of shock reflections from the faces) the situation shown in Fig. 5a is realized in the neighborhood of the wave boundary, and the pressure in the perturbation domain is determined in the symmetric and nonsymmetric cases (the letters s and n in the subscripts) by the formulas

$$P_s^{(1)} = \sin\alpha_1(1 + n + I_1), \; P_n^{(1)} = (1 + n/2)\sin\alpha_1 + (n/2)\sin\alpha_2 + I_2,$$
$$n = 0, 2, 4, \ldots,$$
$$I_1 = I_3 - I_4, \; I_2 = I_3\sin\alpha_2 - I_4\sin\alpha_1, \; I_3 = I\{\sigma^\lambda, \lambda(\theta - \alpha_1), \pi - \lambda\pi/2\}, \tag{7.2}$$
$$I_4 = I\{\sigma^\lambda, \lambda(\theta - \alpha_1), \lambda\pi/2\}$$

(the function I is defined by the relationship (1.4)).

For n = 1, 3, 4, ... (n + 1)/2 ∿ is the quantity of shock reflections from each other), the situation in the neighborhood of the wave boundary is shown in Fig. 5b, and the pressure in the perturbation domain is determined by the formulas

$$P_s^{(1)} = \sin\alpha_1(2 + n + I_1), \; P_n^{(1)} = [(n + 3)\sin\alpha_1 + (n + 1)\sin\alpha_2]/2 + I_2, \; n = 1, 3, 5, \ldots. \tag{7.3}$$

It is interesting that no significant increase in pressure is observed in the perturbation domain as the concave angle moves when $\alpha_1 + \alpha_2 \to 2\pi$, i.e., when the number of weak shock reflections from each other and from the faces of the angle increases. In fact, it can be seen from (7.1)-(7.3) that as $\alpha_1 + \alpha_2 \to 2\pi$ (n large) $P \to \pi M_0/2$ in a linear approximation. Let us note, for comparison, that as a convex angle moves at low velocity, $P \leqslant M_0$ in the perturbation domain in conformity with [4].

Let us establish the nonlinear singularities of the problem in the case of low values of n. In conformity with (7.2) and (7.3), as $r \to 1$ outside the neighborhoods of the triple points B_k, C_k (k = 1, 2)

$$P^{(1)} = P^{(1)}(1, \theta) + Q\rho^{1/2} + O(\rho^{3/2}), \; \rho = 1 - r,$$
$$Q = 2\lambda\sin(\lambda\pi/2)\{\sin\alpha_2/[\cos\lambda(\theta - \alpha_1) + \cos(\lambda\pi/2)] - \sin\alpha_1/[\cos\lambda(\theta - \alpha_1) - \cos(\lambda\pi/2)]\}.$$

Analyzing the sign of Q as a function of θ, we conclude that the fronts A_kB_k, C_1C_2 in Fig. 5 are weak shocks, while the fronts B_1B_2, C_kD_k are lines of weak discontinuity. Their position and parameters in the domains of large gradients, as well as the parameters in the neighborhoods of the triple points B_k, C_k can be determined by formulas from [4].

LITERATURE CITED

1. A. Sakurai, "The flow due to impulsive motion of a wedge and its similarity to the diffraction of a shock wave," J. Phys. Soc. Jpn., 10, No. 3 (1955).

2. W. J. Strang, "A physical theory of supersonic aerofoils in unsteady flow," Proc. Roy. Soc. London, A195, No. 1041 (1948).
3. R. Ya. Tugazakov, "Nonstationary problem of the sudden motion of a wedge and a cone at sub- and supersonic velocities," Uchen. Zapiski TsAGI, 4, No. 1 (1973).
4. V. V. Titarenko, "Nonlinear analysis of the flows initiated by sudden motion of a wedge," Prikl. Mekh. Tekh. Fiz., No. 3 (1976).
5. M. Van Dyke, Perturbation Methods in Fluid Mechanics, Academic, New York (1968).
6. H. Routh, Mechanics of Fluids [Russian translation], Stroiizdat, Moscow (1967).
7. L. Prandtl and O. Tietjens, Applied Hydro- and Aeromechanics, edited by Jacob Den Hartog, Dover (1934).
8. G. Batchelor, Introduction to Fluid Dynamics, Cambridge Univ. Press (1967).
9. A. A. Nikol'skii, "On the "second" form of ideal fluid motion around a streamlined body (investigation of separated vortex flows)," Dokl. Akad. Nauk SSSR, 116, No. 2 (1957).
10. L. I. Sedov, Mechanics of Continuous Medium [in Russian], Vol. 2, Nauka, Moscow (1973).
11. S. M. Belotserkovskii and M. I. Nisht, Separated and Unseparated Ideal Flud Flow around Thin Wings [in Russian], Nauka, Moscow (1978).
12. H. K. Cheng, "Remarks on nonlinear lift and vortex separation," J. Aero. Sci., 21, No. 3 (1954).
13. G. G. Sudakov, "Analysis of the separated flow around a small-span slender triangular wing," Uchen. Zapiski TsAGI, 5, No. 2 (1974).
14. G. M. Arutyunyan and L. V. Karchevskii, Reflected Shocks [in Russian], Mashinostroenie, Moscow (1973).

SELF-SIMILAR PROBLEMS OF THE DYNAMIC BENDING OF INFINITE NONLINEARLY ELASTIC BEAMS

V. P. Yastrebov

UDC 624.07:534.1

Obtaining the exact solutions of dynamic bending problems for beams whose material is not subject to Hooke's law, is fraught with great mathematical difficulties. Approximate methods are used in solving such problems. For instance, the dynamic bending of infinite nonlinearly elastic beams is investigated in [1] by using series expansions of the solution in a variable interval. According to [2, 3], in solving the problem the beam is replaced by a chain of stiff sections interconnected by hinges along the length, wherein elastic or plastic elements with characteristics averaged over the length of each section are concentrated.

In this paper an exact solution on the bending of physically nonlinear infinite beams subjected to concentrated effects is obtained. The beam material is subject to a power-law dependence between the curvature and bending moment. The property of self-similarity of the problem [4, 5] is used to obtain this solution.

1. A homogeneous prismatic beam is considered, whose bending is described by the equation

$$\partial^2 M/\partial x^2 + m\partial^2 w/\partial t^2 = q(x, t), \tag{1.1}$$

where x is a coordinate measured along the beam, t is the time, w is the deflection, M is the bending moment, m is the linear mass of the beam, and q(x, t) is the linear load.

In order to be able to construct a self-similar solution in describing the dependence between the beam curvature and the bending moment, the simplest relationship containing the minimal number of dimensional quantities must be used. The power-law dependence [6]

$$M = M_0(|\partial^2 w/\partial x^2|)^\mu \operatorname{sign}(\partial^2 w/\partial x^2), \tag{1.2}$$

Leningrad. Translated from Zhurnal Prikladnoi Mekhaniki i Tekhnicheskoi Fiziki, No. 4, pp. 165-172, July-August, 1981. Original article submitted May 7, 1980.

 0021-8944/81/2204-0588$07.50